Inorganic Chemistry

Communication

pubs.acs.org/IC

Slow Magnetic Relaxation in Octahedral Cobalt(II) Field-Induced Single-Ion Magnet with Positive Axial and Large Rhombic Anisotropy

Radovan Herchel,[†] Lucia Váhovská,[‡] Ivan Potočňák,[‡] and Zdeněk Trávníček*,[†]

[†]Regional Centre of Advanced Technologies and Materials, Department of Inorganic Chemistry, Faculty of Science, Palacký University, 17. Listopadu 12, CZ-771 46 Olomouc, Czech Republic

[‡]Department of Inorganic Chemistry, Institute of Chemistry, P. J. Šafárik University, Moyzesova 11, SK-04154 Košice, Slovakia

Supporting Information

ABSTRACT: Pseudooctahedral mononuclear cobat(II) complex $[Co(abpt)_2(tcm)_2]$ (**1**), where abpt = 4-amino-3,5-bis(2-pyridyl)-1,2,4-triazole and tcm = tricyanomethanide anion, shows field-induced slow relaxation of magnetization with U = 86.2 K and large axial and rhombic single-ion zero-field-splitting parameters, D = +48(2) cm^{-1} and E/D = 0.27(2) (D = +53.7 cm^{-1} and E/D = 0.29 from ab initio CASSCF/NEVPT2 calculations), thus presenting a new example of a field-induced single-ion magnet with transversal magnetic anisotropy.

There have been a lot of scientific efforts devoted to understanding magnetic exchange and magnetic anisotropy in mono- and polynuclear coordination compounds since the discovery of a new class of molecular magnets exhibiting slow relaxation of magnetization, so-called single-molecule magnets (SMMs).[1] In recent years, a subclass of SMMs emerged from this group, named single-ion magnets (SIMs), where only a single paramagnetic center is present and responsible for SMM-like behavior,[2] thus confirming the dominant role of magnetic anisotropy in SMM design.[3] The key concept of SMM behavior is the existence of a spin-reversal barrier defined as $U = |D|(S^2 - {}^1/_4)$, where S is the half-integer spin of the ground state and D is the axial parameter of zero-field splitting (ZFS), which is supposed to be *negative* in order to observe slow relaxation of magnetization. However, very recently, a few examples of cobalt(II) field-induced SIM compounds have been reported that possess a *positive* D parameter.[4] This behavior is still not completely understood and thus it is wanted to study this phenomenon more thoroughly.

In the reported mononuclear cobalt(II) complex $[Co(abpt)_2(tcm)_2]$ (**1**), the abpt [4-amino-3,5-bis(2-pyridyl)-1,2,4-triazole] and tcm (tricyanomethanide anion) ligands were combined, which resulted in a $\{CoN_6\}$ chromophore with a deformed octahedral geometry (Figure 1), which can be approximated by a slightly compressed octahedron.[5] The crystal structure is stabilized by hydrogen bonds (Figure S1 in the Supporting Information, SI) and $\pi-\pi$ stacking (Figure S2 in the SI), but cobalt(II) atoms are well-separated with an interatomic separation longer than 9 Å, thus excluding pertinent intermolecular magnetic interactions.

Temperature- and field-dependent magnetic data are depicted in Figure 2. The effective magnetic moment μ_{eff} adopts the value of 4.93 μ_B at room temperature, which is significantly higher than

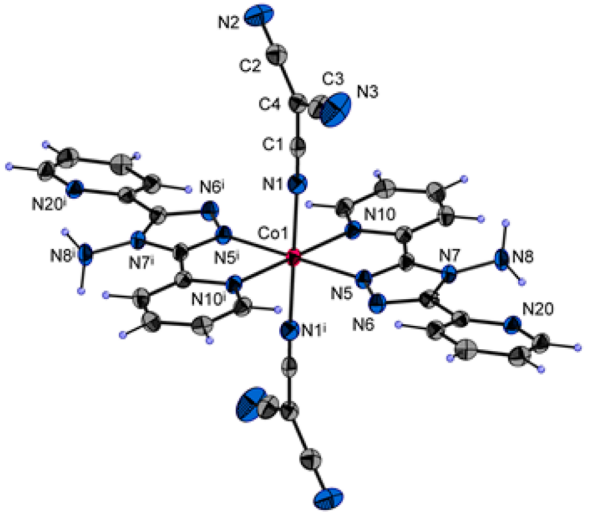

Figure 1. Molecular structure of **1** (ellipsoids at the 50% probability level) together with the atom-labeling scheme. Selected bond lengths and angles (in angstroms and degrees): Co1−N5 = 2.109(2), Co1−N10 = 2.125(2), Co1−N1 = 2.133(2); N10−Co1−N1 = 89.66(6), N5−Co1−N10 = 77.18(6), N5−Co1−N10^i = 102.82(6), N5−Co1−N1 = 87.88(6), N5−Co1−N1^i = 92.12(6), N10−Co1−N1^i = 90.34(6). i = 1 − x, −y, 1 − z.

the spin-only value for $S = {}^3/_2$ and g = 2.0 (μ_{eff}/μ_B = 3.87), pointing to considerable contribution of the orbital angular momentum. μ_{eff}/μ_B continuously decreases upon cooling to a value of 3.75 at T = 2 K, which can be assigned to a large ZFS. The impact of ZFS on the magnetic properties is clearly visible also on isothermal magnetizations measured at T = 2 and 5 K up to 6 T, which differ substantially from the Brillouin function (Figure 2).

In order to interpret the experimental data, the following spin Hamiltonian was postulated:[6]

$$\hat{H} = D(\hat{S}_z^2 - \hat{S}^2/3) + E(\hat{S}_x^2 - \hat{S}_y^2) + \mu_B B g \hat{S}_a \qquad (1)$$

where D and E are the single-ion axial and rhombic ZFS parameters and a defines the orientation of the magnetic field vector $\mathbf{B}_a = B(\sin\theta\cos\varphi, \sin\theta\sin\varphi, \cos\theta)$. The final calculated molar magnetization was calculated as an integral average (eq 2) in order to properly simulate the powder sample signal.

Received: April 18, 2014
Published: May 22, 2014

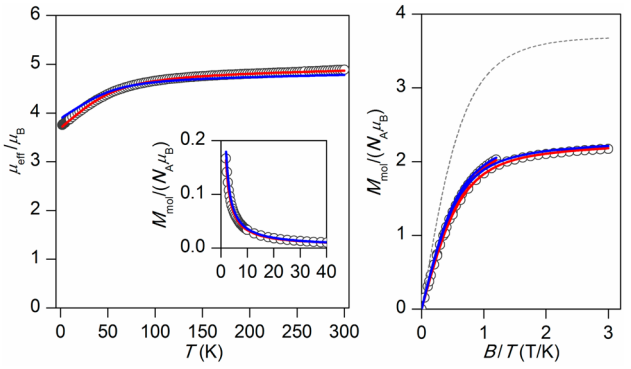

Figure 2. Magnetic data for **1**. Left: temperature dependence of the effective magnetic moment and molar magnetization measured at B = 0.1 T. Right: isothermal magnetizations measured at T = 2 and 5 K. Empty circles: experimental data. Red full lines: calculated data using eq 1, with g = 2.461(6), D = +48(2) cm^{-1}, E/D = 0.27(2) cm^{-1}, and χ_{TIP} = 6.0(7) × 10^{-9} m^3 mol^{-1}. Dashed line: calculated Brillouin function for S = $^3/_2$ and g = 2.461. Blue full lines: calculated data using the CASSCF/NEVPT2 energy levels.

$$M_{mol} = 1/4\pi \int_0^{2\pi} \int_0^{\pi} M_a \sin\theta \, d\theta \, d\varphi \quad (2)$$

It is important to stress that both temperature- and field-dependent magnetization data were fitted simultaneously with the aim to obtain trustworthy parameters. The fitting procedure resulted in a positive axial ZFS parameter and a quite large rhombic ZFS parameter: g = 2.461(6), D = +48(2) cm^{-1}, E/D = 0.27(2), and χ_{TIP} = 6.0(7) × 10^{-9} m^3 mol^{-1} (Figure 2), where χ_{TIP} stands for the contribution of temperature-independent paramagnetism. An alternative fit with the anisotropic **g** tensor resulted in g_{xy} = 2.526(6), g_z = 2.00 (fixed), D = +55(2) cm^{-1}, E/D = 0.27(3), and χ_{TIP} = 13.0(7) × 10^{-9} m^3 mol^{-1} (Figure S3 in the SI). The large magnetic anisotropy is also exhibited in a 3D plot of magnetization (Figure 3). The significant D and E values can be explained as a consequence of both axial and equatorial distortions of the pseudo-octahedral chromophore, which can be quantified either using angular distortions[7] with Σ = 61.1° or using interatomic distances with continuous shape measures,[8] S_{Oh} = 0.855. From chemical point of view, magnetic anisotropy also reflects different nature of nitrogen-donor atoms originated from the triazole ring, pyridine ring and cyanide-group of the tcm ligand.

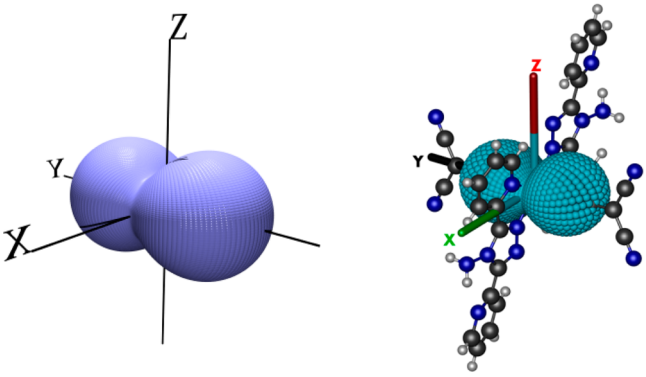

Figure 3. Left: 3D plot of molar magnetization calculated with parameters derived from magnetic analysis: g = 2.461(6), D = +48(2) cm^{-1}, and E/D = 0.27(2) cm^{-1}. Right: molecular structure of **1** overlaid with a 3D plot of molar magnetization derived from the CASSCF/NEVPT2 energy levels with corresponding x, y, and z axes of the **D** tensor. The molar magnetizations in both figures were calculated for T = 2 K and B = 3 T.

To further support our conclusions following from magnetic analysis, we performed ab initio calculations of ZFS parameters based on state-averaged complete-active-space self-consistent-field (SA-CASSCF)[9] wave functions complemented by N-electron valence second-order perturbation theory (NEVPT2)[10] using *ORCA 3.0.1* software.[11] The active space of the CASSCF calculations was composed of seven electrons in five metal-based d orbitals [CAS(7,5)]. The state-averaged approach was used, in which all 10 quartet states and 40 doublets states were equally weighted. The polarized triple-ζ-quality basis set [def2-TZVP(-f)] proposed by Ahlrichs and co-workers was used for cobalt and nitrogen atoms, while the def2-SVP basis set was used for carbon and hydrogen atoms.[12] The calculations utilized the RI approximation with the decontracted auxiliary def2-TZV/C and def2-SVP/C Coulomb fitting basis sets and the chain-of-spheres (RIJCOSX) approximation to exact exchange as implemented in *ORCA*.[13] Increased integration grids (Grid4 in *ORCA* convention) and tight SCF convergence criteria were used in all calculations. The calculations were started with the geometry of the experimentally determined X-ray structure. The ZFS parameters, based on dominant spin−orbit coupling contributions from excited states, were calculated through quasi-degenerate perturbation theory,[14] in which an approximation to the Breit−Pauli form of the spin−orbit coupling operator (SOMF approximation)[15] and the effective Hamiltonian theory[16] were utilized. The resulting values of the ZFS parameter were D = +53.7 cm^{-1} and E/D = 0.29, and they are in good agreement with the values obtained by analysis of the magnetic data [D = +48(2) cm^{-1} and E/D = 0.27(2)]. Furthermore, we used the respective ab initio CASSCF/NEVPT2 spin−orbit coupling, orbital, and spin angular momentum matrices

$$\mathbf{H} = \mathbf{H}_{SOC} + \mu_B(\mathbf{L} + g_e\mathbf{S})\cdot\mathbf{B} \quad (3)$$

to calculate all 120 energy levels for any orientation of magnetic field $\mathbf{B}_a$, followed by integral calculation of both temperature- and field-dependent magnetization data, which are in good agreement with the experimental ones (Figure 2). Inspection of the lowest (2S + 1) energy levels led to the following **g**-tensor parameters: g_x = 2.475, g_y = 2.624, and g_z = 2.022 (Figure S5 in the SI). Moreover, a 3D plot of magnetization, together with the corresponding x, y, and z axes of the **D** tensor related to the molecular structure, is visualized in Figure 3, showing that compression of the octahedron is induced by a small bite angle of the abpt ligand. Alternating-current susceptibility measurement in a nonzero static field, B_{dc} = 0.3 T, shows the characteristic pattern for slow relaxation of magnetization typically observed for SMM species (Figure 4). Analysis of the susceptibility data for each temperature using the one-component Debye model

$$\chi(\omega) = \chi_S + (\chi_T - \chi_S)/[1 + (i\omega\tau)^{1-\alpha}] \quad (4)$$

resulted in isothermal (χ_T) and adiabatic (χ_S) susceptibilities, relaxation times (τ), and distribution parameters (α). This enabled us to construct the Argand (Cole−Cole) plot (Figure 4). Next, we analyzed the temperature dependence of the relaxation time using the expression

$$\tau^{-1} = AB^2T + CT^n + \tau_0^{-1}\exp(-U/kT) \quad (5)$$

dx.doi.org/10.1021/ic500916u | *Inorg. Chem.* 2014, 53, 5896−5898

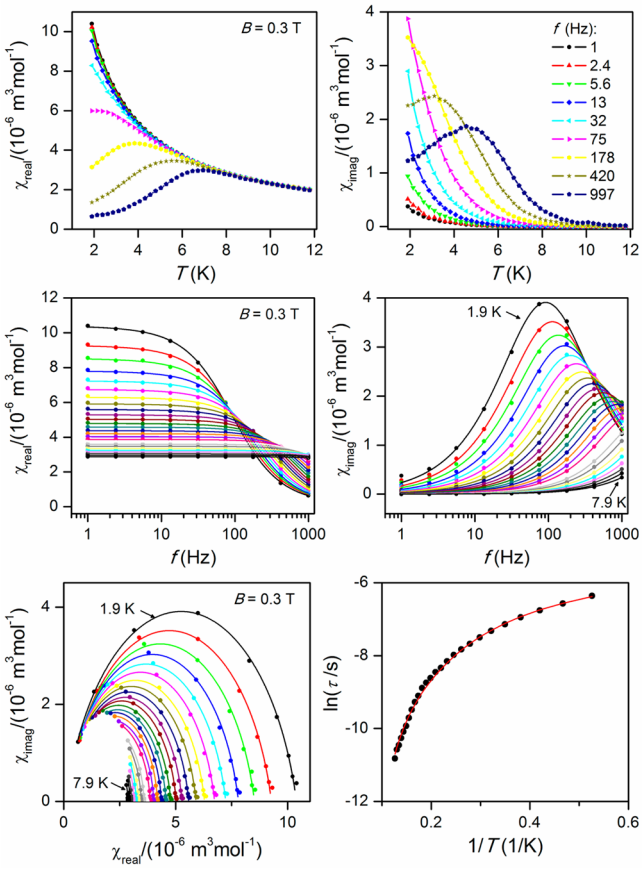

Figure 4. Top: In-phase χ_{real} and out-of-phase χ_{imag} molar susceptibilities for **1** at the applied external field B_{dc} = 0.3 T. Lines serve as guides for the eyes. Middle: Frequency dependence of in-phase χ_{real} and out-of-phase χ_{imag} molar susceptibilities for **1** at B_{dc} = 0.3 T. Full points: experimental data. Full lines: fitted data using eq 4. Bottom: Argand (Cole−Cole) plot and fit of the resulting relaxation times according to eq 5 (red line).

where direct, Raman, and Orbach processes were involved.[2c] The best fit was obtained with the following parameters: $A = 2879\ T^{-2}\ K^{-1}\ s^{-1}$, $C = 7.30\ K^{-4}\ s^{-1}$ for $n = 4$, $\tau_0 = 1.37 \times 10^{-9}\ s^{-1}$, and spin-reversal barrier U = 86.2 K (Figure 4). The value of U is approximately half smaller than the energy separation between the $|\pm^3/_2\rangle$ and $|\pm^1/_2\rangle$ spin states $[U_{theor} = 2(D^2+3E^2)^{1/2}]$ deduced from either magnetic analysis (153 K) or ab initio calculations (172 K). The found spin-reversal barrier U = 86.2 K is the largest among other cobalt(II) field-induced SIMs with transversal anisotropy, $U = 12.7\ cm^{-1}$ in ref 4a, $U = 17.0\ cm^{-1}$ in ref 4b, and $U = 22.6\ cm^{-1}$ in ref 4c, thus showing the potential of this class of SIMs to further increase U even in the case in which the theoretical apparatus to predict its size based on ZFS parameters D and E is still missing.

■ ASSOCIATED CONTENT

Ⓢ Supporting Information

Experimental details, figures and tables referring to synthesis, X-ray analysis, and magnetic data analysis. This material is available free of charge via the Internet at http://pubs.acs.org.

■ AUTHOR INFORMATION

Corresponding Author

*E-mail: zdenek.travnicek@upol.cz. Phone: +420 585 634 352. Fax: +420 585 634 354. Homepage: www.rcptm.com.

Notes

The authors declare no competing financial interest.

■ ACKNOWLEDGMENTS

We acknowledge financial support from these projects: GAČR P207/11/0841, CZ.1.05/2.1.00/03.0058, APVV-00014-11, VEGA 1/0598/14, VVGS-PF-2013-90, and IVF No. 51200545.

■ REFERENCES

(1) Gatteschi, D.; Sessoli, R.; Villain, J. *Molecular Nanomagnets*; Oxford University Press: Oxford, U.K., 2006.

(2) For example, see: (a) Woodruff, D. N.; Winpenny, R. E. P.; Layfield, R. A. *Chem. Rev.* **2013**, *113*, 5110−5148. (b) Zadrozny, J. M.; Atanasov, M.; Bryan, A. M.; Lin, C.-Y.; Rekken, B. D.; Power, P. P.; Neese, F.; Long, J. R. *Chem. Sci.* **2013**, *4*, 125−138. (c) Grigoropoulos, A.; Pissas, M.; Papatolis, P.; Psycharis, V.; Kyritsis, P.; Sanakis, Y. *Inorg. Chem.* **2013**, *52*, 12869−12871. (d) Poulten, R. C.; Page, M. J.; Algarra, A. G.; Le Roy, J. J.; López, I.; Carter, E.; Llobet, A.; Macgregor, S. A.; Mahon, M. F.; Murphy, D. M.; Murugesu, M.; Whittlesey, M. K. *J. Am. Chem. Soc.* **2013**, *135*, 13640−13643.

(3) (a) Waldmann, O. *Inorg. Chem.* **2007**, *46*, 10035−10037. (b) Neese, F.; Pantazis, D. A. *Faraday Discuss.* **2011**, *148*, 229−238.

(4) (a) Zadrozny, J. M.; Liu, J.; Piro, N. A.; Chang, C. J.; Hill, S.; Long, J. R. *Chem. Commun.* **2012**, *48*, 3927−3929. (b) Vallejo, J.; Castro, I.; Ruiz-García, R.; Cano, J.; Julve, M.; Lloret, F.; De Munno, G.; Wernsdorfer, W.; Pardo, E. *J. Am. Chem. Soc.* **2012**, *134*, 15704−15707. (c) Colacio, E.; Ruiz, J.; Ruiz, E.; Cremades, E.; Krzystek, J.; Carretta, S.; Cano, J.; Guidi, T.; Wernsdorfer, W.; Brechin, E. K. *Angew. Chem., Int. Ed.* **2013**, *52*, 9130−9134.

(5) See the SI for the synthesis and characterization of **1** in detail.

(6) Boča, R. *Theoretical Foundations of Molecular Magnetism*; Elsevier: Amsterdam, The Netherlands, 1999.

(7) Angular distortion from an ideal octahedron is calculated as $\Sigma = \Sigma_i^{12}|90 - \alpha_i|$, where α_i stands for 12 *cis* angles of the coordination polyhedron.

(8) (a) Pinsky, M.; Avnir, D. *Inorg. Chem.* **1998**, *37*, 5575−5582. (b) Alvarez, S.; Avnir, D.; Llunell, M.; Pinsky, M. *New J. Chem.* **2002**, *26*, 996−1009.

(9) Malmqvist, P. A.; Roos, B. O. *Chem. Phys. Lett.* **1989**, *155*, 189−194.

(10) (a) Angeli, C.; Cimiraglia, R.; Evangelisti, S.; Leininger, T.; Malrieu, J. P. *J. Chem. Phys.* **2001**, *114*, 10252−10264. (b) Angeli, C.; Cimiraglia, R.; Malrieu, J. P. *Chem. Phys. Lett.* **2001**, *350*, 297−305. (c) Angeli, C.; Cimiraglia, R.; Malrieu, J. P. *J. Chem. Phys.* **2002**, *117*, 9138−9153. (d) Angeli, C.; Borini, S.; Cestari, M.; Cimiraglia, R. *J. Chem. Phys.* **2004**, *121*, 4043−4049. (e) Angeli, C.; Bories, B.; Cavallini, A.; Cimiraglia, R. *J. Chem. Phys.* **2006**, *124*, 054108.

(11) Neese, F. *WIREs Comput. Mol. Sci.* **2012**, *2*, 73−78.

(12) (a) Weigend, F.; Ahlrichs, R. *Phys. Chem. Chem. Phys.* **2005**, *7*, 3297−3305. (b) Schaefer, A.; Horn, H.; Ahlrichs, R. *J. Chem. Phys.* **1992**, *97*, 2571−2577. (c) Schaefer, A.; Huber, C.; Ahlrichs, R. *J. Chem. Phys.* **1994**, *100*, 5829−5835.

(13) Neese, F.; Wennmohs, F.; Hansen, A.; Becker, U. *Chem. Phys.* **2009**, *356*, 98−109.

(14) Ganyushin, D.; Neese, F. *J. Chem. Phys.* **2006**, *125*, 024103.

(15) Neese, F. *J. Chem. Phys.* **2005**, *122*, 034107.

(16) Maurice, R.; Bastardis, R.; Graaf, C.; Suaud, N.; Mallah, T.; Guihéry, N. *J. Chem. Theory Comput.* **2009**, *5*, 2977−2984.